De-tuning a coupled Climate Ice Sheet Model to simulate the North American Ice Sheet at the Last Glacial Maximum

N. Gandy[1,2], L. C. Astfalck[3,2], L. J. Gregoire[2], R. F. Ivanovic[2], V. L. Patterson[2], S. Sherriff-Tadano[2], R. S. Smith[4], D. Williamson[5,6], R. Rigby[2,7]

[1]Department of Natural and Built Environment, Sheffield Hallam University, UK
[2]School of Earth and Environment, The University of Leeds, UK
[3]School of Physics, Mathematics and Computing, The University of Western Australia, Australia
[4]NCAS, Department of Meteorology, University of Reading, Reading, UK
[5]Exeter University, UK
[6]The Alan Turing Institute, UK
[7]Centre for Environmental Modelling and Computation, University of Leeds, Leeds, UK

Key Points:

- Simulating the Last Glacial Maximum Laurentide Ice Sheet with the coupled Climate-Ice Sheet model FAMOUS-ice requires re-tuning
- We efficiently rule out unsuitable parameter values using a Gaussian Process emulator to design waves of short and long simulations
- The different cloud cover between North America and Greenland makes the Last Glacial Maximum a good test for climate-ice-sheet models

Corresponding author: Niall Gandy, `n.gandy@shu.ac.uk`

Abstract

The maximum extent of the last North American ice sheet is well constrained empirically, but it has proven to be challenging to simulate with coupled Climate-Ice Sheet models. Coupled Climate-Ice Sheet models are often too computationally expensive to sufficiently explore uncertainty in input parameters, and it is unlikely values calibrated to reproduce modern ice sheets will reproduce the known extent of the ice at the Last Glacial Maximum. To address this, we run a series of ensembles with a coupled Climate-Ice Sheet model (FAMOUS-ice), simulating the final stages of growth of the last North American Ice Sheets' maximum extent. Using this large ensemble approach, we explore the influence of uncertain ice sheet, albedo, atmospheric, and oceanic parameters on the ice sheet extent. We find that albedo parameters determine the majority of uncertainty when simulating the Last Glacial Maximum North American Ice Sheets. Importantly, different albedo parameters are needed to produce a good match to the Last Glacial Maximum North American Ice Sheets than have previously been used to model the contemporary Greenland Ice Sheet, due to differences in cloud cover over ablation zones. Thus calibrating coupled climate-ice sheet models solely for present day strongly biases simulations of past and future climates different from today.

Plain Language Summary

At the peak of the last ice age, an ice sheet covered much of North America. The extent of this ice sheet is well-understood after decades of intensive data collection, but producing a computer simulation of the ice sheet which matches our observations has been a challenge. This is partly because of uncertainty about the "correct" model set-up to create the best simulation, and partly because the computer models used in the simulations require large computing resources.

In this paper, we present a series of simulations of the North American ice sheet at the peak of the last ice age using a fast-running computer model in which the atmosphere and ice sheets interact. We run hundreds of simulations to tackle the uncertainty about the optimum values for unknown input parameters. We find that the model's representation of how reflective the ice sheet surface is has the most impact on the size and shape of the simulated ice sheet. Importantly, the parameter values that produce the best simulations of modern-day Greenland produce poor simulations of the North American ice sheets during the last ice age, calling into question whether the parameters chosen for modern Greenland will produce reasonable simulations of future ice sheet change and sea level rise.

1 Introduction

Accurately estimating future changes in ice sheets is crucial for producing meaningful projections of future sea level rise (IPCC, 2021). Ice sheets interact with the atmosphere and ocean, and are vulnerable to instabilities in their growth and retreat (e.g. Shepherd et al., 2012; J. Gregory et al., 2012). These instabilities, along with the uncertainties in processes of climate and ice sheet evolution, make future projections using numerical models difficult, and the accuracy of any future simulations is a challenge to assess. For the Greenland ice sheet, one of the main sources of uncertainty is the future changes in surface mass balance (the balance of accumulation and melt of snow and ice at the surface) (Fettweis et al., 2011). This surface mass balance is highly dependent on both the climate and the ice sheet topography, as well as the strong interactions between the two. Thus projections of future Greenland evolution need to account for climate-ice sheet interactions (Goelzer et al., 2017). However, there are major challenges in representing surface mass balance and climate ice sheet interactions in models: (i) climate models often have large biases in ice sheet regions (Davy & Outten, 2020), (ii) these regions are difficult environments to work in, limiting the observations we have of the climate and surface mass balance (Vernon et al., 2013) and (iii) surface melt occurs in narrow steep regions at the edge of the ice sheets that are difficult processes to capture or represent in global climate models.

Major progress has been made to tackle these challenges and there are now several earth system models that include interactive ice sheets in Greenland and/or Antarctica (e.g. Danabasoglu et al., 2020; R. S. Smith et al., 2021). However, there are numerous challenges in simulating climate-ice sheet interactions. Perhaps most acutely, there is a mismatch of spatial and temporal scales between typical ice sheet and global climate models. Spatially, kilometer (or sub-kilometer) processes are important for accurate simulation of ice sheet processes, such as grounding line migration, and margin precipitation gradients (Franco et al., 2012; Cornford et al., 2013), so recent ice sheet models have been developed to simulate ice sheets at this scale, e.g. through adaptive mesh refinement, and they require climate (or surface mass balance inputs) at that scale. On the other hand, Atmosphere Ocean General Circulation Models (AOGCMs) have a grid-box size 10-1000× larger than the scale of modelled ice sheet processes and inputs (Sellar et al., 2019; Danabasoglu et al., 2020). This conundrum of mistmatching scales is flipped in the time domain. Temporally, AOGCMs require sub-daily timesteps to accurately simulate the climate system, while ice sheet change is usually a multi-centennial process. The spatial-temporal mismatch of scales creates a problem for computational efficiency, since high resolution is needed for both and isn't easily compromised for one in favour of the other. Consequently, most AOGCMs cannot practically simulate interactive ice sheet change, instead prescribing the ice sheet extent as a boundary condition (e.g. Kageyama et al., 2017; Ivanovic et al., 2015; Menviel et al., 2019) and updating the ice sheet periodically for palaeo runs where significant ice sheet change occurs. Similarly, ice sheet simulations often rely on prescribed climate or surface mass balance fields (e.g. L. J. Gregoire et al., 2016; Patton et al., 2013; Gandy et al., 2021).

Nonetheless, recent technical advances have allowed coupled simulations of the climate and ice sheets, through a combination of model development and increasing compute power. The spatial mismatch between ice sheet and climate model grids can be addressed by calculating ice-sheet relevant processes, such as albedo calculations, with subgridscale parameterisations (Ganopolski et al., 2010; Vizcaíno et al., 2013; Ziemen et al., 2014; R. S. Smith et al., 2020, 2021). One way to solve the problem of time scale (subdaily timesteps for multimillennial integrations) is to couple the ice sheet to climate models which are typically computationally efficient, in part due to having relatively low spatial resolution, meaning the the simulations can be run for the length of time needed to spin-up and simulate the co-evolution of ice sheets and climate.

A remaining challenge is how coupled climate-ice sheet models should be calibrated and tested. For many models, uncertain parameters are hand-tuned to produce stable modern ice sheets of the right shape and size compared to observations. However, this only represents one point in time. The recent past, for which we have direct observations of ice sheets has seen relatively small changes compared to those expected in the next centuries. These observations thus provide poor constraints on the strength of climate-ice sheet feedbacks and there is a danger of over-fitting the model to modern conditions and compensating for biases in the simulated climate. To have confidence in the ability of coupled climate-ice sheet models we need to test them under conditions different from today where we have sufficient observational constraints on the climate and ice sheets.

We propose to use the Last Glacial Maximum as a benchmark for coupled climate-ice sheet models. This period, which occurred around 21,000 years ago, has been a focus of the Palaeoclimate Model Intercomparison Project since the 1990s (Kageyama, Abe-Ouchi, et al., 2021), because it was a period of relatively stable and well documented climate, with CO2 concentrations much lower than today (180 ppm). The North American ice sheet is thought to have reached a relatively stable maximum extent, that is very well reconstructed (e.g. Dyke et al., 2002; Peltier et al., 2015; Gowan et al., 2021). It is thus possible to run equilibrium simulations under LGM conditions with an interactive North American ice sheet until a stable maximum ice extent is reached, which can be meaningfully compared to reconstructions. Ice at the LGM reached much lower latitudes than today, providing a way to test the ability of models to represent SMB and climate-ice interactions under energy balance conditions different than modern Greenland.

We use FAMOUS-Ice (R. S. Smith et al., 2020), a coarse resolution, fast running AOGCM, which has been used in long-palaeo simulations (R. S. Smith, 2012; J. Gregory et al., 2012; Roberts et al., 2014; Dentith et al., 2019; L. J. Gregoire et al., 2012) and uncertainty quantification (L. Gregoire et al., 2010), coupled to the Glimmer Ice Sheet model by downscaling SMB calculations (R. S. Smith et al., 2020), rather than previous work using a PDD SMB scheme (J. Gregory et al., 2012). This coupled model has been used to simulate present and future Greenland Ice Sheet evolution (J. M. Gregory et al., 2020). We start the manuscript by presenting the first attempt at simulating the LGM with the FAMOUS-ice model with interactive ice sheets in Greenland and North America. Here, we use an atmosphere-only version of FAMOUS, prescribing Sea Surface Temperatures (SSTs) and Sea Ice Concentrations (SICs) in order to minimise biases in surface climate. We found that with the standard tuning that reproduced the modern Greenland shape and size (R. S. Smith et al., 2020) the model produces a collapse of the North American ice sheet under LGM climatic conditions. We then present the efficient method we developed to generate large ensembles of coupled climate ice sheet simulations simultaneously varying uncertain parameters controlling the climate, ice sheet and surface mass balance. Finally we show that albedo parameters are the primary control on uncertainty in our ensemble and we investigate the link between, cloudiness, albedo and surface mass balance under modern and glacial conditions.

2 Model description and setup

FAMOUS-ice is a fast climate model coupled to the Glimmer ice sheet model (R. S. Smith et al., 2020). The atmospheric component is that of FAMOUS, a fast low resolution general circulation model designed for running simulations of the climate on multi-millennial timescales (e.g. Dentith et al., 2019; L. J. Gregoire et al., 2012) and large ensembles for calibration or uncertainty quantification purposes (L. Gregoire et al., 2010). The Glimmer ice sheet model is a fast simplified 3D dynamical ice sheet model based on the shallow ice approximation that is used to simulate continental ice sheets over glacial interglacial cycles (L. J. Gregoire et al., 2015; Rutt et al., 2009). A multilayer surface snow scheme is used in the atmosphere model to calculate surface mass balance (SMB) at ten different elevation levels within each grid cell that contains part of an ice sheet. The SMB calculated by the atmosphere model is regridded from the coarse FAMOUS-ice grid (7.5°longitude by 5°latitude) onto the surface of the Glimmer ice sheet model (in this case $40km \times 40km$) each model year. The use of ten elevation levels on which SMB is calculated provides a mean to effectively "downscale" the SMB from the coarse atmospheric grid to the finer ice sheet grid. Coupled climate-ice sheet simulations would usually be too computationally expensive to run as part of large multi-millennial ensembles, but the speed of both FAMOUS and Glimmer make these experiments possible.

During the development of FAMOUS-ice, albedo parameters were manually tuned to simulate a stable Greenland ice sheet at present day (R. S. Smith et al., 2020). The model has been applied to evaluate the long-term future decline of the Greenland Ice Sheet (J. M. Gregory et al., 2020). In both cases, sea surface temperatures and sea ice concentrations in FAMOUS were prescribed from the output of higher resolution and complexity climate models to allow some control of the climate evolution and reduce the impact of biases resulting from atmosphere-ocean and sea ice interactions. FAMOUS can also be used with a dynamical ocean (e.g. Dentith et al., 2019) and the Glimmer ice sheet component can be replaced with the more complex and computationally expensive BISICLES ice sheet model (Cornford et al., 2013; Matero et al., 2020; Gandy et al., 2018).

We setup FAMOUS-ice to simulate the climate of the Last Glacial Maximum, with interactive North American and Greenland ice sheets. We follow the PMIP4 LGM protocol (Kageyama et al., 2017) to setup most of the climate boundary conditions, including the CO_2, CH_4, and N_2O concentrations. Global orography and the land-sea mask was taken from the 21 ka BP Glac-1D reconstruction (Tarasov et al., 2012b), and preindustrial (PI) vegetation distribution was implemented and kept constant throughout the run. Thus our simulation neglect the effects of climate-ice-vegetation feedbacks that can affect ice sheet evoluation (Stone & Lunt, 2013). The orbital configuration is set to 23 ka BP, rather than 21 ka BP as in the PMIP4 protocol. This is 2,000 years prior to the ice sheet maximum extent to represent an orbit closer to point of maximum volume for the North American Ice Sheet (Peltier et al., 2015; Tarasov et al., 2012b). This slightly inhibits ice sheet growth as shown by a sensitivity experiment included in the supplementary information.

SSTs and sea ice concentrations are taken from the statistical reconstruction of Astfalck et al. (2021), combining information from the PMIP LGM multi-model ensemble (Kageyama, Harrison, et al., 2021) and compilations of proxy data (Kucera et al., 2005), and their associated uncertainties. The method is able to generate ensembles of plausible SST and SIC pairs that can be used to drive atmosphere models. The simulated SSTs are in good agreement with the proxy-based reconstruction of Paul et al. (2021) with significantly warmer tropical SSTs than the data assimilation product of Tierney et al. (2020).

The interactive ice sheet model domain is set to cover North America, Greenland, and Iceland. All other ice sheets are fixed to match the Glac-1D reconstruction. The Glimmer initial condition is taken from a previous ensemble of North American Ice Sheet deglaciations (L. J. Gregoire et al., 2016); specifically, ensemble member *Cano3-022* at 18.2 ka BP. This was chosen to represent an intermediate sized ice sheet resembling the likely extent during Marine Isotope Stage 3 (Gowan et al., 2021), from which to grow the North American ice sheet to an equilibrium ice sheet volume. In FAMOUS-ice, ice is able to grow by flowing onto a gridcell not previously covered in ice, but ice is not able to form from the accumulation of snow into an unglaciated gridcell. We thus chose an initial condition with a Cordilleran ice sheet. We also chose to start with ice already covering the Hudson Bay as the Glimmer ice sheet model does not represent the complex processes of grounding line migration. Simulations are run with 10 $\times$ ice sheet acceleration; i.e., for every climate year simulated, Glimmer integrates for 10 ice sheet years with the same surface mass balance inputs (from the climate model). After this, the new Glimmer ice sheet surface elevation is passed back to the climate model, regridded and processed to update its orography and ice fraction fields.

We first run an initial standard experiment, using the atmosphere model parameters from simulations that produce a stable contemporary Greenland ice sheet (J. M. Gregory et al., 2020) (apart from boundary conditions altered according to the PMIP4 LGM protocol), and ice sheet model parameters from previous simulations of the North American ice sheet with glimmer (L. J. Gregoire et al., 2016). Parameters that may have an impact on the ice sheet evolution are listed in Table 1.

3 Collapse of the LGM ice sheet with a standard setup

Unexpectedly, with the the standard parameter values from (R. S. Smith et al., 2020), instead of growing from a mid-glacial ice sheet size, the North American ice sheet rapidly deglaciates in our standard experiment, losing half its volume in 2,500 years. This eventually results in a simulation with LGM climate conditions, but no North American Ice Sheet (Figure 1). The deglaciation is driven by ablation across the North American Ice

Table 1. Key climate and ice sheet parameters in the simulation

Parameter	Standard Value	Ensemble Range	Units	Notes
Lapse rate	6	2-10	$K\ km^{-1}$	Prescribed lapse rate for air temperature used to downscale FAMOUS near-surface ice sheet climate onto surface elevation tiles. Downwelling longwave radiation is also adjusted for consistency
Daice	-0.35	-0.4-0	K^{-1}	Sensitivity of bare-ice albedo to surface air temperatures once the surface is in a melt regime
AVGR	0.007	0.001-0.01	μm^{-1}	Sensitivity of the snow albedo to variation in surface grain size
Fsnow	600	350-800	$kg\ m^{-3}$	The threshold in surface snow density at which the FAMOUS albedo scheme switches from a scattering paradigm appropriate for a conglomeration of snow grains to one more appropriate for a solid surface
Flow factor	3	1-10		The softness of ice. Increasing the factor makes the ice softer and more deformable
Mantle relaxation time	3000	500-9000	yr	The relaxation time of the mantle, a lower value essentially making the mantle less viscous, thus allowing a quicker topographic rebound.
Basal sliding	10	0.5-20	$mm\ yr^{-1}$ Pa^{-1}	The basal sliding rate. A higher value allows increased ice velocity.
RHCRIT	0.85	0.6-0.9		The threshold of relative humidity for cloud formation (R. Smith, 1990).
VF1	1.882	1-2	ms^{-1}	The precipitating ice fall-out speed (Heymsfield, 1977).
CT	0.000302	5×10^{-5}-4×10^{-4}	s^{-1}	The conversion rate of cloud liquid water droplets to precipitation (R. Smith, 1990).
CW	0.001688	0.0001-0.002	$kg\ m^{-3}$	The threshold values of cloud liquid water for formation of precipitation (R. Smith, 1990). Only the value for the land is varied.
Entrainment rate	3	1.5-6		Entrainment rate coefficient Convection Scales rate of mixing between environmental air and convective plume.
Alpham	0.2152	0.2-0.65		The sea ice low albedo (Crossley & Roberts, 1995).

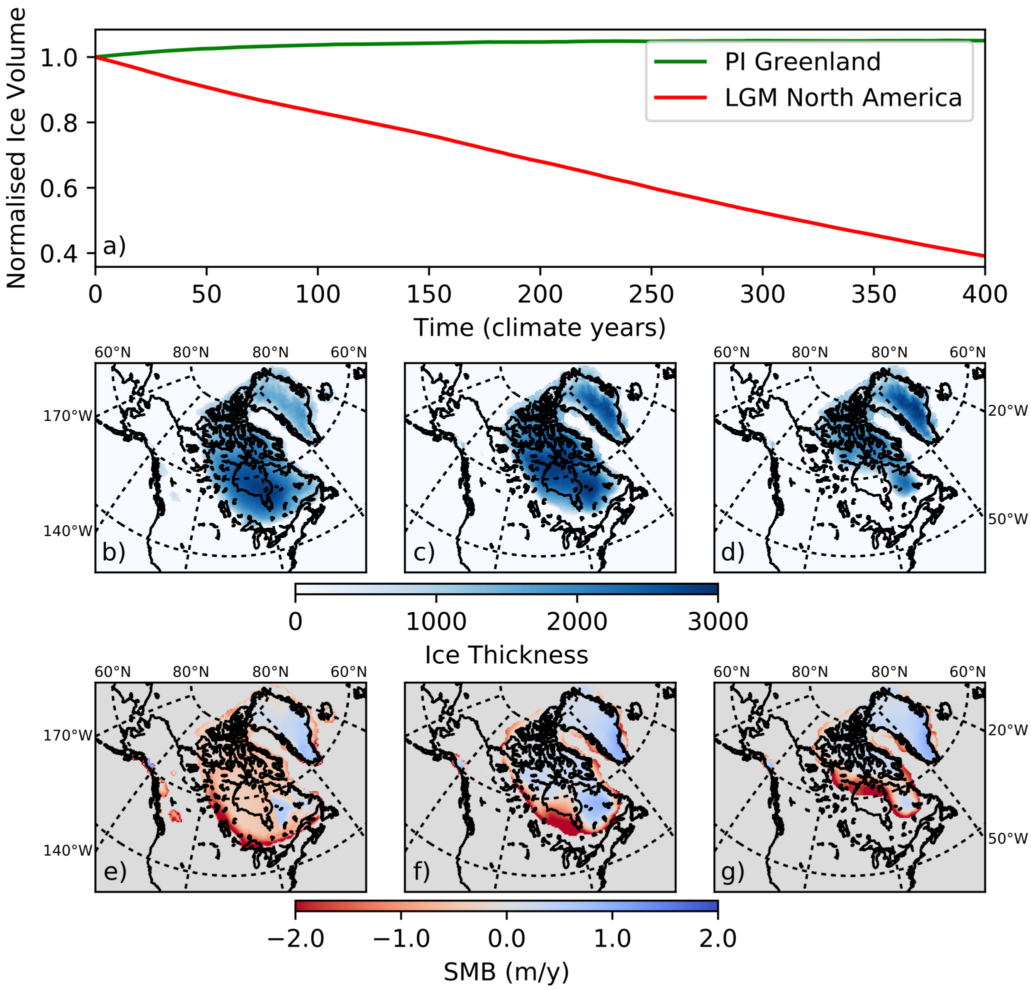

Figure 1. LGM North American Ice Sheet evolution in the standard setup. a) The ice sheet volume, normalised by the initial volume (green line) compared to the PI Greenland simulations (red line). b-d) Ice Thickness at 0, 2000 and 4000 years into the run. e-g) The SMB at 0, 2000 and 4000 years into the run.

Sheet, including the ice sheet interior (Figure 1e), which is present from the start of the simulation and causes a rapid retreat of the southern margin northward through Hudson Bay (Figure 1b-d). The Greenland Ice Sheet on the other hand maintains its initial extent, which corresponds to full glacial conditions, in good agreement with observations (Simpson et al., 2009).

We know from geologic constraints (Dyke et al., 2002) that the ice sheet should be considerably larger than simulated here (i.e. it should cover the whole of Canada). We therefore conclude that parameters previously tuned to simulate the present day Greenland ice sheet well (as in (R. S. Smith et al., 2020)) are not suitable for the LGM North American Ice Sheet. To find a reasonable simulation, we thus need to fully explore the uncertainty in model input parameters controlling the surface mass balance, ice sheet dynamics and climatic conditions over the ice sheets in FAMOUS-ice as described be-low, in essence to "de-tune" the model and find parameter combinations that produce good representations of the LGM North American Ice Sheet.

4 The Ensemble Approach

4.1 An Initial Pass: Wave 1

We started by running a large 280-member ensemble of simulations varying parameter values of Table 1. These values were sampled using k-extended Latin Hypercube sampling (Williamson, 2015) within ranges derived from previous uncertainty quantification work with FAMOUS (L. Gregoire et al., 2010) and Glimmer (L. J. Gregoire et al., 2016), with the addition of the Entrainment rate coefficient. We purposefully chose wide but plausible ranges (Table 1) with the aim to identify a region of the parameter space that would produce a reasonable North American ice extent at the LGM. We expected that similar to the standard simulation (Section 3), many runs would fully deglaciate. Thus, to optimise our use of computing resources, simulations were stopped at 2,500, 5,000, and 10,000 ice sheet years if they lost more than 25% of the initial ice sheet area.

In the majority of the 280 ensemble members, the North American ice volume reduces dramatically and thus all but 18 simulations were terminated early (figure 2a). However, five simulations remain relatively stable at the initial volume and area, and ice volume grows in twelve simulations. This deglaciation could be caused by errors in the simulated climate. We thus compared the ensemble results to prior simulations from PMIP3 and PMIP4 (Figure 3). We find that global mean temperature is broadly in line with previous PMIP3 and PMIP4 simulations - on the warmer end around 284K. The range of global mean temperatures in the ensemble is limited by the prescribed SSTs, which have a variability in the temperatures spatial distribution, but the same global mean SST (within 0.5K).

To assess our ice sheet results, we compare them to the ice extent reconstructed by Dyke et al. (2002). We calculate ice extent error as in Gregoire et al. (2016); by summing up the number of gridcells where the ice does not match the reconstruction. The maximum allowed error extent was chosen to align with the maximum LGM extent error from the NROY ensemble of L. J. Gregoire et al. (2016). L. J. Gregoire et al. (2016) applied a cumulative extent error over the whole deglaciation to identify their NROY set of simulations, we translated this into a maximum bound for our LGM extent error metric by applying our metric to their final NROY set and identifying the maximum value obtained. Constraints on North American ice volume are not as well known as ice extent, but can provide a useful metric for ruling out simulations. We chose to set a minimum threshold of 2.1 $\times 10^7 km^3$ for ice volume as in L. J. Gregoire et al. (2016), based on a variety of individual reconstructions (Clark & Tarasov, 2014; Lambeck et al., 2014; Peltier et al., 2015; Tarasov et al., 2012a). Only a small subset of the simulations (18 out of 280) terminate the simulation within this accepted criteria for volume and extent, highlighted by the green box in Figure 2b. We refer to the parameters of these simulations as Not Ruled Out Yet (NROY).

The average spatial extent of the ensemble is a poor fit to reconstructed ice extent (Figure 2c). Very few simulations approach the southern margin. In fact, despite stopping deglaciating simulations early only around 40% of simulations cover Hudson Bay, which should be in the ice sheet interior. Of the 18 simulations that do have a larger extent, there is a variety of ice configurations, but some consistent model-data mismatch. All the ice sheets that grow from the initial extent include extensive ice in Alaska, which was mostly ice free at the LGM (Dyke et al., 2002). After this first wave of 280 runs, more simulations were required to determine if these errors are systematic in the model setup, or an artefact of the small number of simulations with a larger ice sheet volume.

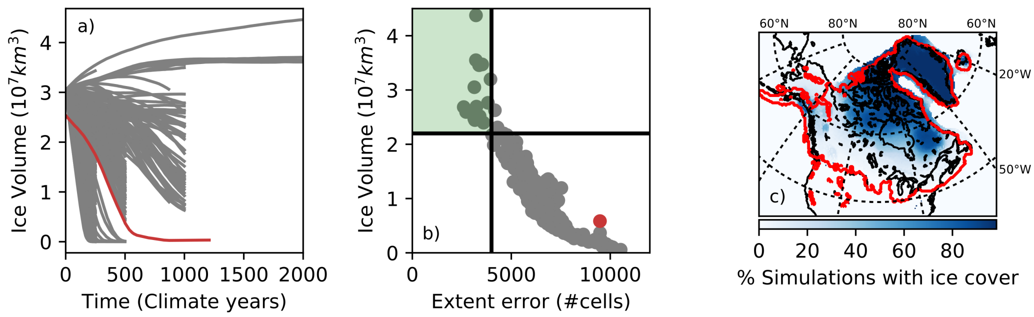

Figure 2. Wave 1 of the ensemble. a) North American Ice volume evolution for each ensemble member. b) The final ice volume and extent error (compared to the Dyke et al. (2002) margin) for each ensemble member. c) The % of simulations with ice cover compared to the Dyke et al. (2002) margin. The red line and point on panels a and b shows the control run, as shown in Figure 1.

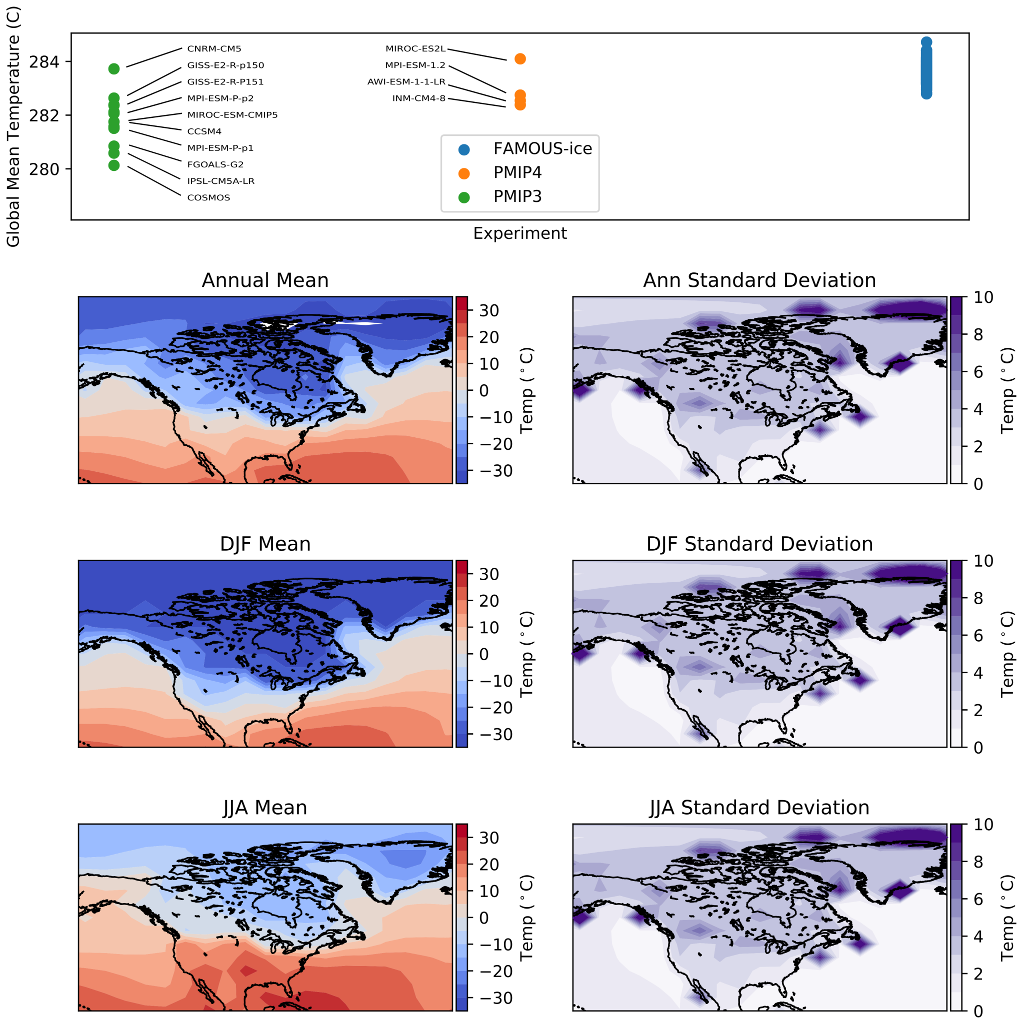

Figure 3. The surface temperature climatology of the Wave 1 ensemble compared to previous simulations as part of PMIP3 and PMIP4.

4.2 Refining the Ensemble: Wave 2

The fact that only 18 of 280 simulations in Wave 1 sustain a large enough North American ice sheet indicates that the majority of the parameter space, defined in Table 1, produce inappropriate conditions for the maintenance of a North American Ice Sheet. Searching through the parameter space to find realistic simulations thus required the use of statistical emulation and an intelligent and efficient iterative ensemble design to identify and target the space of 'reasonable' parameters. In order to provide optimal (parameter) space coverage of the design, whilst respecting the simulations that are already run, we use a stratified k-extended Latin Hypercube design (details follow).

Reaching an equilibrium in ice volume requires long simulations, particularly for the good simulations that take 10,000 years to reach a reasonable ice volume (Figure 4). In order to reduce computational cost, we investigated if it was possible to guess whether a simulation would be good or bad based on information from the start of the simulation. For the ice sheet to grow to a glacial maximum volume, it needs to accumulate more snow than the snow and ice lost in the ablation zone. In other words, the surface mass balance (SMB) at least needs to be positive. This is a conservative minimum requirement; in reality an ice sheet with a positive SMB may not reach the target reconstructed LGM extent, but this requirement excludes simulations that certainly cannot reach the target extent.

To efficiently select inputs for Wave 2 we generate a candidate set of runs by first identifying, from Wave 1, initial SMB values that result in plausible equilibrium ice-sheet areas; and second, emulating these initial SMB values as a function of the input parameters. We identified a strong relationship between the equilibrium ice-sheet area and the average SMB value from the first 20 years. Denote by b the 20 year averaged SMB value, and by A the "equilibrium" ice-sheet area after 10,000 ice sheet years. A predictive model of equilibrium ice-sheet area takes the form $A = f(b)+\epsilon$ where $f(\cdot)$ may be any function. We considered f to be either linear or a Gaussian process and found that the linear model gave more conservative in the uncertainty estimates, which was desired as we want the Wave 2 runs to bound the NROY space. Define a predictive interval $P(b) = [f(b) + 3\sqrt{\text{var}(\epsilon)}, f(b) - 3\sqrt{\text{var}(\epsilon)}]$ from our predictive model. We target equilibrium ice-sheet areas in the interval $T = [1.5 \times 10^7 km^2, 2 \times 10^7 km^2]$ and consider the b (and the corresponding input parameters) such that the intersection $P(b) \cap T$ is non-zero as plausible for design in Wave 2.

To find combinations of input parameters that produce plausible values of b (and hence equilibrium ice-sheet areas), we ran three sub-waves of 20 year-long simulations to obtain the average SMB in the first 20 years. Note that simulations in the fist sub-wave were run for 50 years to examine relationships other than 20-year SMB average that, in the end, were not used. Running these shorter simulations is still somewhat costly, and so we utilised a Gaussian Process (GP) emulator to design for parameterisations that was likely to produce desirable values for b. Define by x the multivariate vector of parameters that we build the emulator over: here x comprised of the 4 most influential parameters `FSNOW`, `AVGR`, `DAICE`, and `FLOW FACTOR` (see Table 1). We model b via a stochastic GP, $b \sim \mathcal{GP}(x)$, where the effects of the parameters not explicitly represented in x is handled by the stochasticity of the process. The specific set-up of this GP is provided in code as supplementary material.

From our three sub-waves of 20-50 year-long simulations, we are able to extract a candidate set of simulations for the Wave 2 ensemble. The first sub-wave (Wave 1.1) samples 200 ensemble members, which are predicted from the emulator to have non-negligible probability of positive SMB. This results in around 50% of simulations in this subwave having a positive SMB, an increase from 15% in the original wave (Figure 4b, Wave 1.1). We attempt to refine the predictive bounds on the GP model twice more (Figures 4c-d, Wave 1.2 and 1.3), with no improvement. This is likely due to the inherent stochas-

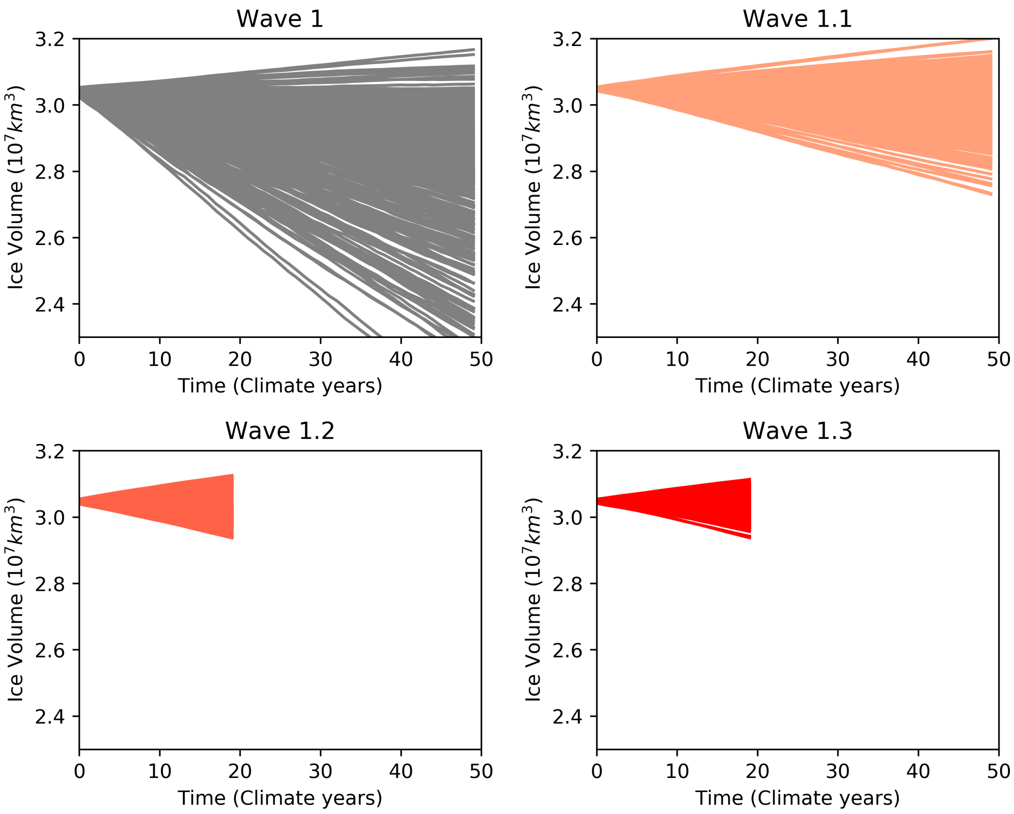

Figure 4. Ice Volumes simulated in the successive ensemble subwaves of simulations sampled to have a positive initial surface mass balance using the Gaussian Process emulator.

ticity of the climate model and cumulative effects of the parameters that we absorb into the predictive error term. At the end of this process of iterative short waves, our candidate set contains over 1000 20-year long simulations that have a positive SMB over the North American ice sheet. From this candidate set, we select an optimal (with respect to space-filling and accounting for the previous Wave 1 runs) design of 200 ensemble members to continue for a full 10,000 years to an equilibrium North American Ice Sheet. These 200 simulations make up our Wave 2. For context, this process of GP model subwaves saved around 230,000 core hours (or about 2 months of real time) compared to running a full second ensemble wave.

4.3 Wave 2 Results

By sampling a second wave of long simulation from the shorter subwaves, we design an ensemble of simulations that produce more NROY ice sheet extents, with 120/200 simulations maintaining or growing volume beyond the initial extent (Figure 5a). 176 more simulations out of the 200 wave 2 simulation are considered to be NROY based on the volume and extent error thresholds previously described (Figure 5b), a factor of ten increase from the 18 out of 280 simulations in Wave 1. This demonstrates the success of our approach in efficiently identifying good combinations of parameters values. Some simulations (56/200) shrank in volume slightly, but expended in area to meet both the volume and area constraints to be considered NROY. The definition of an NROY ensemble member is lenient, but could be further constrained (for example, by adding a target for the top of the atmosphere energy balance) depending on future research questions or aims.

The mean ice sheet extent of the second wave is close to the southern ice sheet margin (Figure 5c). However, simulations that meet this margin still show some consistent model-data mismatch. All simulations with a low Laurentide Ice Sheet extent error have ice that is too extensive in Alaska. This is also common in ice sheet-only simulations with Glimmer (L. J. Gregoire et al., 2016; Ji et al., 2021) driven by climate forcing from FAMOUS and from the higher resolution CCSM3 model, so is likely a systematic bias resulting from the climate model. Alaskan ice extent was limited by the wider ice sheet disrupting atmospheric circulations (Löfverström & Liakka, 2016; Tulenko et al., 2020). The likelihood of matching observations is not helped by the climate coupling; a low resolution of FAMOUS struggles to simulate the temperature and precipitation gradients caused by steep topography such as the Aleutian Range (Abe-Ouchi et al., 2007). Prescribing the SMB forcing in an uncoupled model nudges the simulated ice sheets towards the ice sheet prescribed (usually from reconstructions) in the climate-only model, encouraging a better match between modelled and reconstructed ice geometry, but not necessarily for predictive reasons. Instead, in this case, a coupled climate-ice sheet model essentially introduces additional freedom into the simulations to produce a greater variety of ice sheets.

At this point, we could repeat the subwave emulation step from the first wave of simulations in an attempt to further narrow the parameter range and produce a third wave of simulations with a greater proportion of NROY simulations. However, this second wave has already produced 176 more NROY simulations, and running large waves of simulations is computationally costly. We deem that there would be diminishing benefits to running subsequent waves of simulations beyond this point.

5 Importance of Albedo Values

While 13 parameters are varied in the ensemble, it is clear that only three to four of these parameters explain the majority of the variation in the model outputs. This is demonstrated in Figure 6, where the parameter ranges for Wave 1 and Wave 2 are compared. In Wave 2, the statistical emulator has removed regions of the parameter space that do not produce reasonable ice sheet extents. There are large changes to the ranges of FSNOW, DAICE, and AVGR, in the NROY ensemble, but limited changes for the other ten parameters.

The parameters that are most influential on the simulated ice sheet volume all control the ice sheet surface albedo, these are the snow-ice density threshold (FSNOW), the maximum albedo of bare ice (DAICE), and the snow grain size (AVGR) (Table 1, see Smith et al 2020 for full details of how these terms are used in their respective parameterisations). As expected, the largest ice volumes result from having more reflective snow and bare ice (from AVGR and DAICE respectively), and a high density threshold (FSNOW) to start considering snow to be ice (keeping a surface classed as more reflective snow, rather than ice, for longer). The average surface albedo of the NROY simulations is 0.1 higher than from the ruled-out simulations (Figure 5).

5.1 Why does the ice sheet deglaciate at low albedos?

We have shown that albedo parameters that have been manually tuned to produce a reasonable contemporary Greenland ice sheet (J. M. Gregory et al., 2020; R. S. Smith et al., 2020) produce a collapsed North American Ice Sheet at the LGM. Here, we explore the reasons why the present day Greenland ice sheet may not be a sufficient target for calibrating a coupled climate-ice sheet model. The contrasting behaviour between present day Greenland and North American LGM ice sheets is associated with differ-

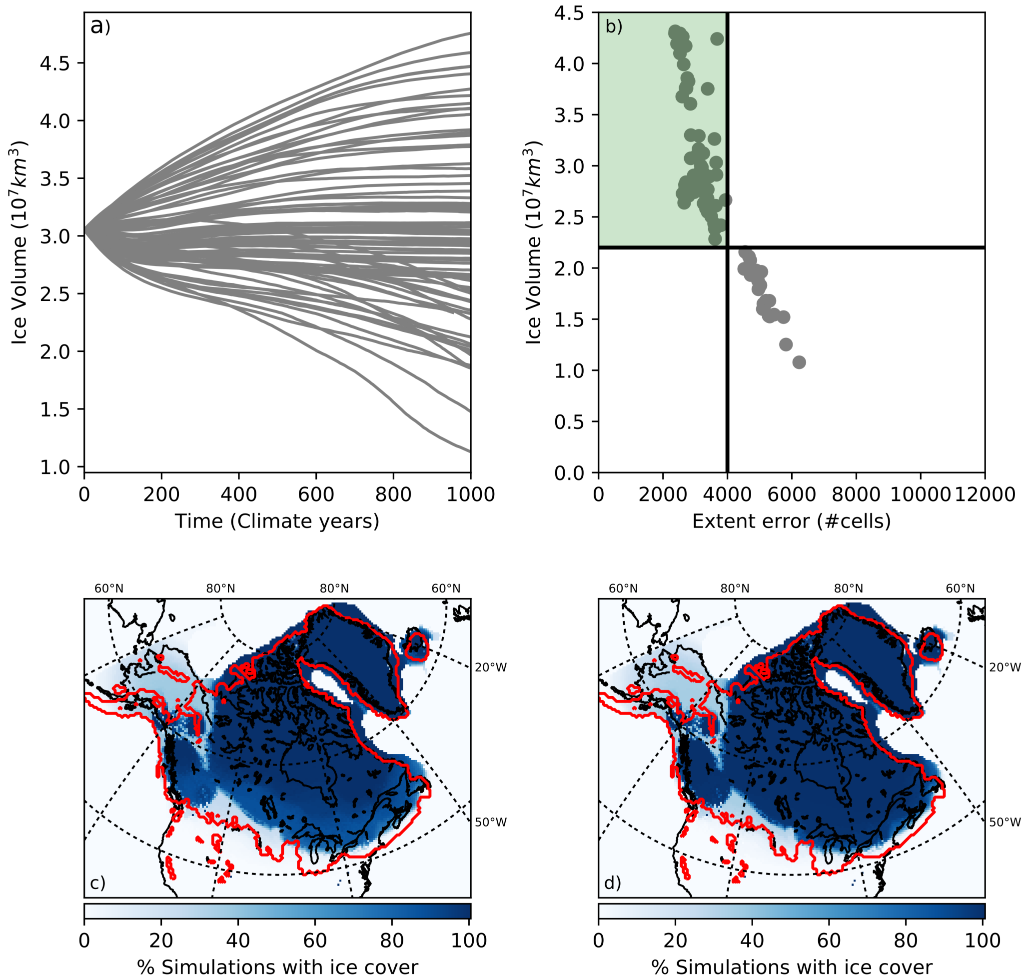

Figure 5. Wave 2 of the ensemble. a) Ice volume evolution for each ensemble member. b) The final ice volume and extent error (compared to the Dyke et al. (2002) margin) for each ensemble member. The % of simulations with ice cover shown as shades of blue compared to the Dyke et al. (2002) margin plotted as the red contour for the whole Wave 2 ensemble (c), and just for the NROY members of the Wave 2 ensemble (d).

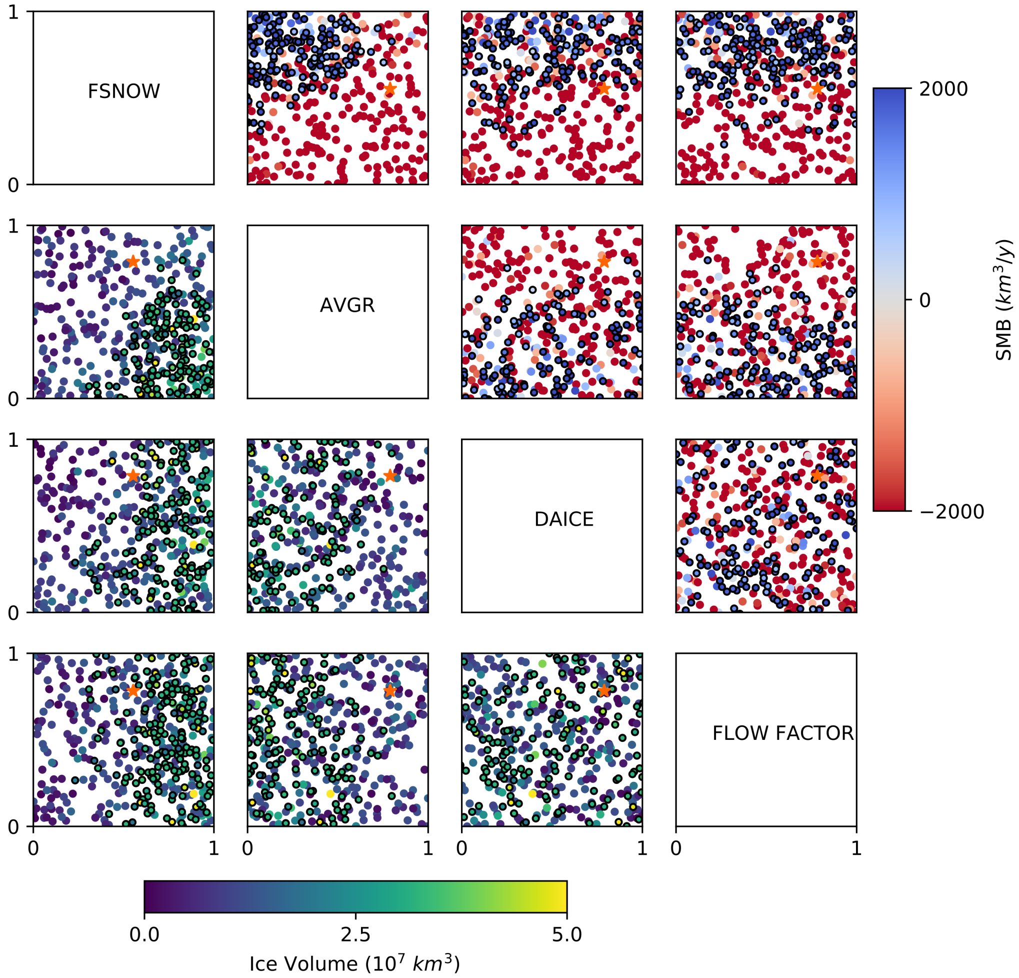

Figure 6. The resulting initial 20-year SMB and equillibrium Ice Volumes as a function of normalised albedo and flow factor parameter combinations in the ensembles. Wave 2 ensemble members are circled in black, and are clustered in the parameter space as a result of the GP emulator aiming for a positive SMB. For reference, the control simulation is marked by an orange star.

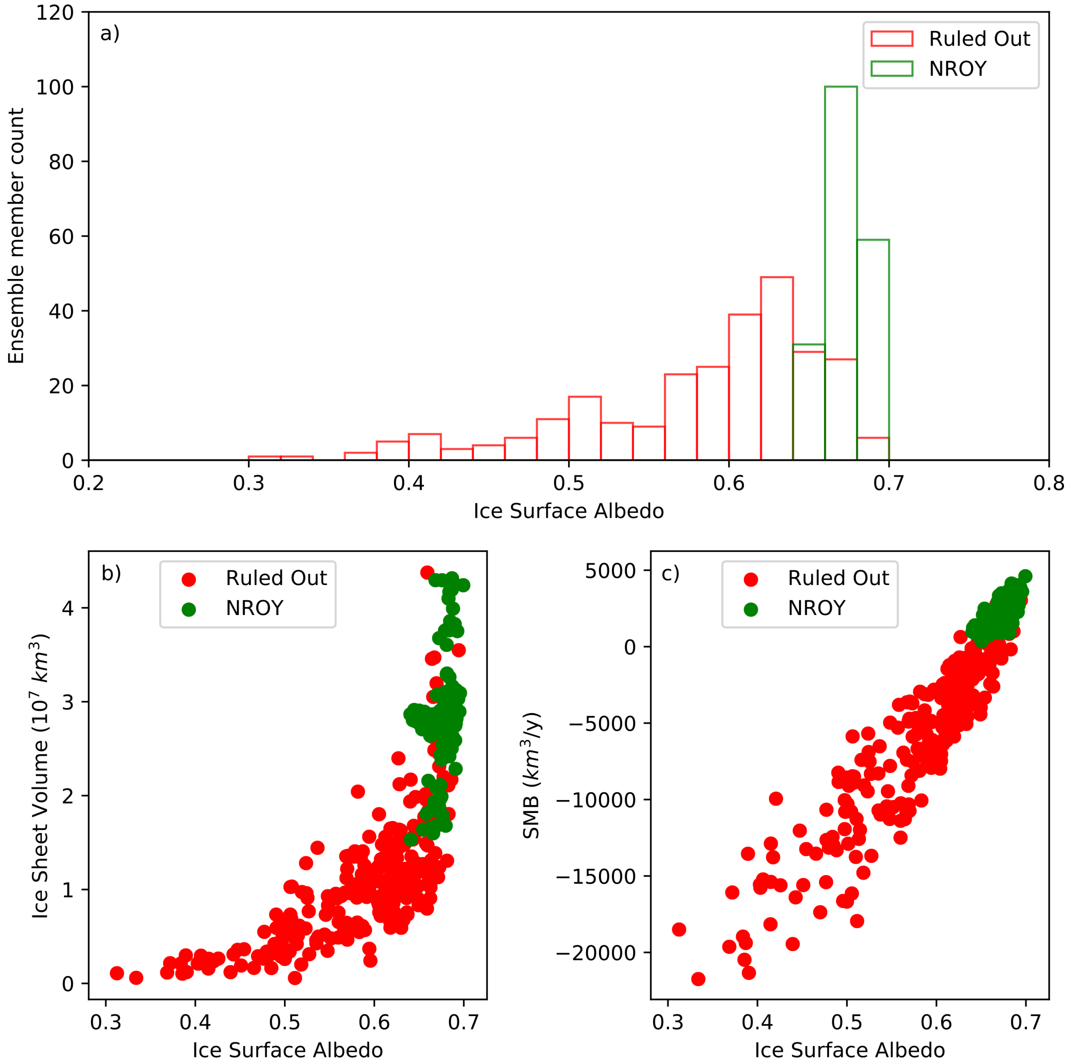

Figure 7. Average Ice Sheet surface albedos for NROY and Ruled Out ensemble members across both Wave 1 and Wave 2. a) The distribution of ice surface albedos for NROY and Ruled Out ensemble members. b) The relationship between final ice sheet volume and the ice sheet surface albedo. c) The relationship between the 30-year ice sheet SMB and the ice sheet surface albedo. All ice sheet surface albedos are taken as a 30-year average of the July albedo at the start of a simulations, so that ice sheet extents are comparable between ensemble members.

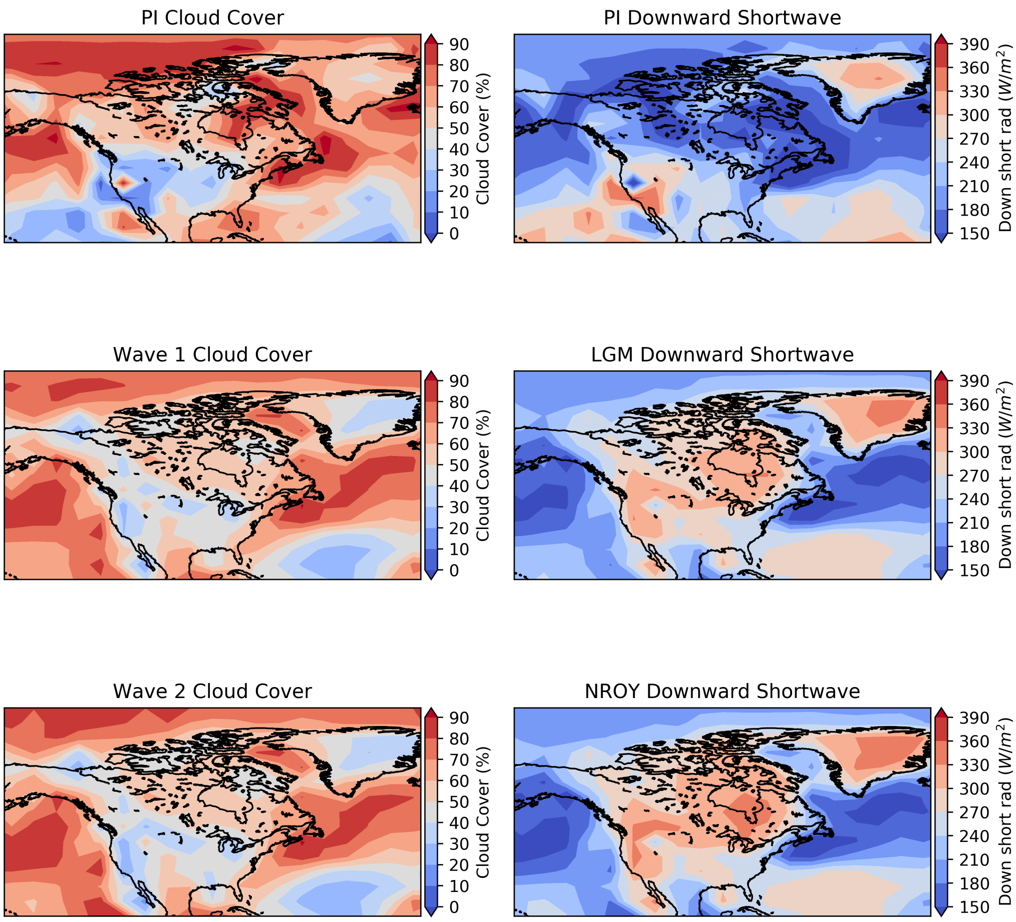

Figure 8. July cloud cover and downward shortwave radiation for the PI simulation, Wave 1, and Wave 2.

ences in the magnitude of downward shortwave radiation at surface and cloud cover between the two ice sheets. In the modern Greenland simulations, the ablation zone at the ice sheet margin is often covered by thick clouds (Figure 8).

Simply, the relationship between cloud and ice sheet surface albedo can be split into three groups (Figure 9). At high surface elevations there is lower temperatures and cloud cover; a "sunny cold" regime that can sustain an ice sheet. At lower elevations there can be sufficient cloud cover to reduce downward shortwave radiation, and therefore limit ice sheet melt. In this "cloudy warm" regime the cloud cover means the ice sheet is insensitive to its surface albedo. Finally, at lower elevations and limited cloud cover we can see a "sunny warm" regime, where the ice sheet is highly sensitive to surface albedo parameters. Figure 9 shows downward shortwave radiation and ice surface albedo values for each ice sheet surface gridbox in the control runs for PI Greenland and LGM North America. While both runs occupy the "sunny cold" and "cloudy warm" regime, the "sunny warm" regime is dominated by the LGM run. In this manner, the North American ice sheet becomes very sensitive to low ice albedo parameters.

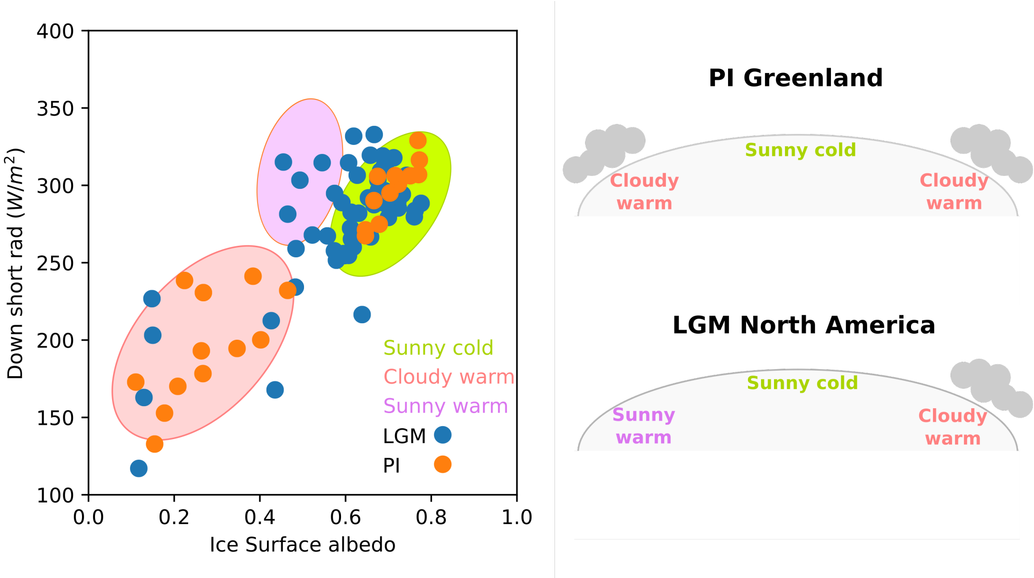

Figure 9. Comparison of energy balance between LGM North American and modern Greenland ice sheets: a) Downward Shortwave radiation vs ice surface albedo in each ice sheet gridcell for Greenland in the "standard" pre-industrial simulation (orange) and for the North American ice sheet in the "standard" LGM simulation (blue). Shaded ovals show the proposed surface albedo and radiation behaviour groups for the Greenland and Laurentide Ice Sheets. b) A schematic of the different radiative effect of clouds on the PI Greenland and LGM Laurentide Ice Sheets.

We further examine outputs from PMIP3 models (Brady et al., 2013; Voldoire et al., 2013; Ullman et al., 2014; Sueyoshi et al., 2013; Adloff et al., 2018) to verify whether the very strong downward shortwave radiation over the North American ice sheet observed in FAMOUS-ice is a common feature among other models. The area-averaged values over the North American ice sheet are summarised in Table 2. The results show that other PMIP models simulate stronger downward shortwave radiation at the southern margin of the ice sheet, and that FAMOUS-ice shows the smallest value for this together with CCSM4 (Table 2). In other words, other models may impose an even stronger melt on the ice sheet than in our simulations. This is associated with the strongest cloud radiative effect in shortwave radiation in FAMOUS-ice and CCSM4. These results show that the North American ice sheet would also be sensitive to low albedo values in other PMIP models; if they allow a very small minimum bare ice albedo, a very large amount of solar energy would be absorbed. Therefore, the larger sensitivity of the LGM North American ice sheet to low albedo parameters is likely not a unique feature of FAMOUS-ice, but seems to be a common feature among other climate models.

There is a large uncertainty and variety in minimum ice sheet surface albedo among PMIP models ranging from 0.2 in MRI and FAMOUS-ice to 0.7 in MPI (Alder & Hostetler, 2019). These differences in albedo values are induced by the combined effects of discrepancies in the physics of the albedo scheme and biases in AGCMs. For the latter, biases in cloud radiative effects (R. S. Smith et al., 2020) and horizontal resolution (Kapsch et al., 2021) can affect the choice of albedo values. Importantly, the albedo values selected are often strongly tuned to reproduce the modern SMB. This is sensible when the focus is on future change of Greenland ice sheet in the next few decades, since changes in SMB are the dominant driver on this time scale. However, ice sheets evolve (e.g. in response to climate) over much longer timeframes, and on a longer time-scale, when the

Table 2. Albedo and radiative characteristics of PMIP3 models and FAMOUS-ice. FAMOUS-ice values are taken from the Wave 2 ensemble, showing the mean value and ensemble range (in brackets).

PMIP3 Model	Surface albedo	Sfc down s/w radiation	Absorbed s/w at sfc
FAMOUS-ice	0.68 (0.56-0.75)	296 (265-324)	96 (71-126)
CCSM4	0.70	295.18	87.40
CNRM	0.34	307.67	204.47
GISS	0.66	341.52	116.34
IPSL	0.75	343.80	86.58
MIROC	0.75	351.76	86.51
MPI	0.83	348.92	58.07
MRI	0.57	318.19	138.25

ice sheet is subject to larger instabilities and more pronounced climate interactions, tuning the albedo parameters may cause an unrealistic relationship between surface albedo and cloud cover. Moreover, changes in the clouds over the next century could have pronounced effects on SMB with unrealistic surface albedo.

In the case of FAMOUS-ice, the surface albedo parameters used for the contemporary Greenland ice sheet were originally tuned to a low value to compensate for an excessive reflection of shortwave radiation by clouds (R. S. Smith et al., 2020). This was performed to better simulate a stable and realistic Greenland ice sheet geometry under modern day climate. However, the resulting ice albedo parameter sets are too low to produce a realistic North American ice sheet at the LGM due to the different cloud cover and downward shortwave radiation over the ablation zone. Therefore we are in an undesirable situation where a model with good SMB in modern climate is unable to simulate the LGM North American Ice Sheets, and could also be unable to simulate other ice sheets and time periods. This result suggests that overtuning the albedo to compensate for biases in other components under modern climate may cause degraded simulation results under different climate states, when the cloud properties and downward shortwave radiation over ablation zones are different from modern. Most concerning, this suggests that simulations projecting the future of the Greenland ice sheet are particularly vulnerable to uncertain future cloudiness over the ice sheet.

6 Conclusions

We have applied a new coupled Climate-Ice Sheet model (FAMOUS-ice) to simulate the maximum extent of the last North American Ice Sheets. The standard model setup manually tuned for modern day Greenland resulted in a collapsed ice sheet at the LGM. We underwent a process of “detuning” the model, running hundreds of simulations to produced a range of reasonable equilibrium ice sheets, enabling us to explore the influence and importance of key uncertain parameters. Large parts of the parameter space produced collapsed ice sheets at the LGM. Efficiently scanning the parameter space for good input parameter combinations thus required an iteration of short simulations informed by emulation of equilibrium ice volume as a function of initial surface mass balance. The results show that FAMOUS-ice is able to simulate the maximum extent of the LGM North American Ice Sheet, with particularly good match to the southern Laurentice limits, though some systematic ice overgrowth remains in Alaska.

From our results, we are able to identify that the parameters controlling ice sheet surface albedo dominate the simulated variability in ice sheet geometry. Importantly, combinations of albedo parameter values that produced a reasonable contemporary Greenland ice sheet do not necessarily produce a reasonable LGM North American Ice Sheet. This is because albedo parameter can be overtuned to compensate for biases in modern clouds over Greenland. The different cloud distribution over the Southern Laurentide ice sheet at the Last Glacial Maximum provide a useful "stress test" for coupled climate-ice sheet models. This highlights the potential problems of relying solely on contemporary observations for model tuning. Efforts to find a region of the parameter space that produce reasonable simulations of contemporary and glacial ice sheets are important, and could lead to improved confidence in future ice sheet projections.

Author Contributions

Niall Gandy (principle researcher - climate ice sheet modelling): Methodology, Software, Investigation, Formal Analysis, Data Curation, Writing - Original Draft, Visualization. Lachlan Astfalck (co-researcher - statistics): Methodology, Software, Investigation, Formal Analysis, Writing - Original Draft. Lauren Gregoire (principle investigator): Conceptualization, Methodology, Writing - Review and Editing, Supervision, Project Administration, Funding Acquisition. Ruza Ivanovic (co-investigator - climate modelling): Conceptualization, Writing - Review and Editing, Supervision. Violet Patterson (contributing researcher - 21 ka orbital simulation): Investigation. Sam Sherriff-Tadano (contributing researcher - albedo and cloud analysis): Investigation, Formal analysis, Writing - Original Draft. Robin Smith (collaborator - climate-ice sheet modelling): Methodology, Software, Writing - Review and Editing. Daniel Williamson (co-investigator - statistics): Methodology, Writing - Review and Editing, Supervision. Richard Rigby (software scientist): Software.

Data Availability

Output from a Wave 2 simulation is archived online (10.17632/8kswwpnjyz.1). All the other simulations can be accessed by contacting the author.

Acknowledgments
NG, LJG, LA, RFI, VLP, DW, and RR were funded by "SMB-Gen" UKRI Future Leaders Fellowship MR/S016961/1. RFI, RSS and SST were funded by "RiSICMAP", NERC Standard Grant NE/T007443/1. This work was undertaken on ARC4, part of the High Performance Computing Facilities at the University of Leeds.

References

Abe-Ouchi, A., Segawa, T., & Saito, F. (2007). Climatic conditions for modelling the northern hemisphere ice sheets throughout the ice age cycle. *Climate of the Past*, *3*(3), 423–438.
Adloff, M., Reick, C. H., & Claussen, M. (2018). Earth system model simulations show different feedback strengths of the terrestrial carbon cycle under glacial and interglacial conditions. *Earth System Dynamics*, *9*(2), 413–425.
Alder, J. R., & Hostetler, S. W. (2019). The dependence of hydroclimate projections in snow-dominated regions of the western united states on the choice of statistically downscaled climate data. *Water Resources Research*, *55*(3), 2279–2300.
Astfalck, L., Williamson, D., Gandy, N., Gregoire, L., & Ivanovic, R. (2021). Coexchangeable process modelling for uncertainty quantification in joint climate reconstruction. *arXiv preprint arXiv:2111.12283*.

Brady, E. C., Otto-Bliesner, B. L., Kay, J. E., & Rosenbloom, N. (2013). Sensitivity to glacial forcing in the ccsm4. *Journal of Climate*, *26*(6), 1901–1925.

Clark, P. U., & Tarasov, L. (2014). Closing the sea level budget at the last glacial maximum. *Proceedings of the National Academy of Sciences*, *111*(45), 15861–15862.

Cornford, S. L., Martin, D. F., Graves, D. T., Ranken, D. F., Le Brocq, A. M., Gladstone, R. M., ... Lipscomb, W. H. (2013, jan). Adaptive mesh, finite volume modeling of marine ice sheets. *Journal of Computational Physics*, *232*(1), 529–549. Retrieved from `http://linkinghub.elsevier.com/retrieve/pii/S0021999112005050` doi: 10.1016/j.jcp.2012.08.037

Crossley, J., & Roberts, D. (1995). Thermodynamic/dynamic sea–ice model. *Meteorological Office, Bracknell*.

Danabasoglu, G., Lamarque, J.-F., Bacmeister, J., Bailey, D., DuVivier, A., Edwards, J., ... others (2020). The community earth system model version 2 (cesm2). *Journal of Advances in Modeling Earth Systems*, *12*(2).

Davy, R., & Outten, S. (2020). The arctic surface climate in cmip6: status and developments since cmip5. *Journal of Climate*, *33*(18), 8047–8068.

Dentith, J. E., Ivanovic, R. F., Gregoire, L. J., Tindall, J. C., & Smith, R. S. (2019). Ocean circulation drifts in multi-millennial climate simulations: the role of salinity corrections and climate feedbacks. *Climate Dynamics*, *52*(3), 1761–1781.

Dyke, A., Andrews, J., Clark, P., England, J., Miller, G., Shaw, J., & Veillette, J. (2002). The laurentide and innuitian ice sheets during the last glacial maximum. *Quaternary Science Reviews*, *21*(1-3), 9–31.

Fettweis, X., Belleflamme, A., Erpicum, M., Franco, B., & Nicolay, S. (2011). *Estimation of the sea level rise by 2100 resulting from changes in the surface mass balance of the greenland ice sheet.* Intech, Croatia.

Franco, B., Fettweis, X., Lang, C., & Erpicum, M. (2012). Impact of spatial resolution on the modelling of the greenland ice sheet surface mass balance between 1990–2010, using the regional climate model mar. *The Cryosphere*, *6*(3), 695–711.

Gandy, N., Gregoire, L. J., Ely, J. C., Clark, C. D., Hodgson, D. M., Lee, V., ... Ivanovic, R. F. (2018, nov). Marine Ice Sheet Instability and Ice Shelf Buttressing Influenced Deglaciation of the Minch Ice Stream, Northwest Scotland. *The Cryosphere*, *12*(July), 1–24. Retrieved from `https://www.the-cryosphere.net/12/3635/2018/https://www.the-cryosphere-discuss.net/tc-2018-116/` doi: 10.5194/tc-2018-116

Gandy, N., Gregoire, L. J., Ely, J. C., Cornford, S. L., Clark, C. D., & Hodgson, D. M. (2021). Collapse of the last eurasian ice sheet in the north sea modulated by combined processes of ice flow, surface melt, and marine ice sheet instabilities. *Journal of Geophysical Research: Earth Surface*, *126*(4), e2020JF005755.

Ganopolski, A., Calov, R., & Claussen, M. (2010). Simulation of the last glacial cycle with a coupled climate ice-sheet model of intermediate complexity. *Climate of the Past*, *6*(2), 229–244.

Goelzer, H., Robinson, A., Seroussi, H., & Van De Wal, R. S. (2017). Recent progress in greenland ice sheet modelling. *Current climate change reports*, *3*(4), 291–302.

Gowan, E. J., Zhang, X., Khosravi, S., Rovere, A., Stocchi, P., Hughes, A. L., ... Lohmann, G. (2021). A new global ice sheet reconstruction for the past 80 000 years. *Nature communications*, *12*(1), 1–9.

Gregoire, L., Valdes, P., & Payne, T. (2010). Sensitivity of last glacial maximum ice sheet modelling to uncertainty in climate forcing. In *Egu general assembly conference abstracts* (p. 9492).

Gregoire, L. J., Otto-Bliesner, B., Valdes, P. J., & Ivanovic, R. (2016, sep). Abrupt

Bølling warming and ice saddle collapse contributions to the Meltwater Pulse 1a rapid sea level rise. *Geophysical Research Letters*, *43*(17), 9130–9137. Retrieved from http://doi.wiley.com/10.1002/2016GL070356 doi: 10.1002/2016GL070356

Gregoire, L. J., Payne, A. J., & Valdes, P. J. (2012, jul). Deglacial rapid sea level rises caused by ice-sheet saddle collapses. *Nature*, *487*(7406), 219–222. Retrieved from http://www.nature.com/articles/nature11257 doi: 10.1038/nature11257

Gregoire, L. J., Valdes, P. J., & Payne, A. J. (2015, nov). The relative contribution of orbital forcing and greenhouse gases to the North American deglaciation. *Geophysical Research Letters*, *42*(22), 9970–9979. Retrieved from http://doi.wiley.com/10.1002/2015GL066005 doi: 10.1002/2015GL066005

Gregory, J., Browne, O., Payne, A., Ridley, J., & Rutt, I. (2012). Modelling large-scale ice-sheet–climate interactions following glacial inception. *Climate of the Past*, *8*(5), 1565–1580.

Gregory, J. M., George, S. E., & Smith, R. S. (2020). Large and irreversible future decline of the greenland ice sheet. *The Cryosphere*, *14*(12), 4299–4322.

Heymsfield, A. J. (1977). Precipitation development in stratiform ice clouds: A microphysical and dynamical study. *Journal of Atmospheric Sciences*, *34*(2), 367–381.

IPCC. (2021). *Ocean, cryosphere and sea level change. in climate change 2021: The physical science basis. contribution of working group i to the sixth assessment report of the intergovernmental panel on climate change* [Book]. Cambridge, United Kingdom and New York, NY, USA: Cambridge University Press. doi: 10.1017/9781009157896.011

Ivanovic, R., Gregoire, L., Kageyama, M., Roche, D., Valdes, P., Burke, A., ... Tarasov, L. (2015). Transient climate simulations of the deglaciation 21–9 thousand years before present; pmip4 core experiment design and boundary conditions. *Geoscientific Model Development Discussions*, *8*, 9045–9102.

Ji, W., Robel, A., Tziperman, E., & Yang, J. (2021). Laurentide ice saddle mergers drive rapid sea level drops during glaciations. *Geophysical Research Letters*, *48*(14), e2021GL094263.

Kageyama, M., Abe-Ouchi, A., Obase, T., Ramstein, G., & Valdes, P. (2021). Modeling the climate of the last glacial maximum from pmip1 to pmip4. *Past Global Changes Magazine*, *29*(2), 80–81.

Kageyama, M., Albani, S., Braconnot, P., Harrison, S. P., Hopcroft, P. O., Ivanovic, R. F., ... others (2017). The pmip4 contribution to cmip6–part 4: Scientific objectives and experimental design of the pmip4-cmip6 last glacial maximum experiments and pmip4 sensitivity experiments. *Geoscientific Model Development*, *10*(11), 4035–4055.

Kageyama, M., Harrison, S. P., Kapsch, M.-L., Lofverstrom, M., Lora, J. M., Mikolajewicz, U., ... others (2021). The PMIP4 Last Glacial Maximum experiments: preliminary results and comparison with the PMIP3 simulations. *Climate of the Past*, *17*(3), 1065–1089.

Kapsch, M.-L., Mikolajewicz, U., Ziemen, F. A., Rodehacke, C. B., & Schannwell, C. (2021). Analysis of the surface mass balance for deglacial climate simulations. *The Cryosphere*, *15*(2), 1131–1156.

Kucera, M., Rosell-Melé, A., Schneider, R., Waelbroeck, C., & Weinelt, M. (2005). Multiproxy approach for the reconstruction of the glacial ocean surface (margo). *Quaternary Science Reviews*, *24*(7-9), 813–819.

Lambeck, K., Rouby, H., Purcell, A., Sun, Y., & Sambridge, M. (2014). Sea level and global ice volumes from the last glacial maximum to the holocene. *Proceedings of the National Academy of Sciences*, *111*(43), 15296–15303.

Löfverström, M., & Liakka, J. (2016). On the limited ice intrusion in alaska at the lgm. *Geophysical Research Letters*, *43*(20), 11–030.

Matero, I. S., Gregoire, L. J., & Ivanovic, R. F. (2020). Simulating the early holocene demise of the laurentide ice sheet with bisicles (public trunk revision 3298). *Geoscientific Model Development*, *13*(9), 4555–4577.

Menviel, L., Capron, E., Govin, A., Dutton, A., Tarasov, L., Abe-Ouchi, A., ... others (2019). The penultimate deglaciation: protocol for paleoclimate modelling intercomparison project (pmip) phase 4 transient numerical simulations between 140 and 127 ka, version 1.0. *Geoscientific Model Development*, *12*(8), 3649–3685.

Patton, H., Hubbard, A., Glasser, N. F., Bradwell, T., & Golledge, N. R. (2013, jul). The last Welsh Ice Cap: Part 2 - Dynamics of a topographically controlled icecap. *Boreas*, *42*(3), 491–510. Retrieved from http://doi.wiley.com/10.1111/j.1502-3885.2012.00301.x doi: 10.1111/j.1502-3885.2012.00301.x

Paul, A., Mulitza, S., Stein, R., & Werner, M. (2021). A global climatology of the ocean surface during the last glacial maximum mapped on a regular grid (glomap). *Climate of the Past*, *17*(2), 805–824.

Peltier, W. R., Argus, D., & Drummond, R. (2015). Space geodesy constrains ice age terminal deglaciation: The global ice-6g_c (vm5a) model. *Journal of Geophysical Research: Solid Earth*, *120*(1), 450–487.

Roberts, W. H., Valdes, P. J., & Payne, A. J. (2014). Topography's crucial role in heinrich events. *Proceedings of the National Academy of Sciences*, *111*(47), 16688–16693.

Rutt, I. C., Hagdorn, M., Hulton, N., & Payne, A. (2009). The glimmer community ice sheet model. *Journal of Geophysical Research: Earth Surface*, *114*(F2).

Sellar, A. A., Jones, C. G., Mulcahy, J. P., Tang, Y., Yool, A., Wiltshire, A., ... others (2019). Ukesm1: Description and evaluation of the uk earth system model. *Journal of Advances in Modeling Earth Systems*, *11*(12), 4513–4558.

Shepherd, A., Ivins, E. R., A, G., Barletta, V. R., Bentley, M. J., Bettadpur, S., ... Zwally, H. J. (2012, nov). A reconciled estimate of ice-sheet mass balance. *Science (New York, N.Y.)*, *338*(6111), 1183–9. Retrieved from http://www.ncbi.nlm.nih.gov/pubmed/23197528 doi: 10.1126/science.1228102

Simpson, M. J., Milne, G. A., Huybrechts, P., & Long, A. J. (2009). Calibrating a glaciological model of the greenland ice sheet from the last glacial maximum to present-day using field observations of relative sea level and ice extent. *Quaternary Science Reviews*, *28*(17-18), 1631–1657.

Smith, R. (1990). A scheme for predicting layer clouds and their water content in a general circulation model. *Quarterly Journal of the Royal Meteorological Society*, *116*(492), 435–460.

Smith, R. S. (2012, feb). The FAMOUS climate model (versions XFXWB and XFHCC): description update to version XDBUA. *Geoscientific Model Development*, *5*(1), 269–276. Retrieved from https://www.geosci-model-dev.net/5/269/2012/ doi: 10.5194/gmd-5-269-2012

Smith, R. S., George, S., & Gregory, J. M. (2020). Famous version xotzb (famous-ice): a gcm capable of energy-and water-conserving coupling to an ice sheet model. *Geoscientific Model Development Discussions*, 1–25.

Smith, R. S., Mathiot, P., Siahaan, A., Lee, V., Cornford, S. L., Gregory, J. M., ... others (2021). Coupling the uk earth system model to dynamic models of the greenland and antarctic ice sheets. *Journal of Advances in Modeling Earth Systems*, *13*(10), e2021MS002520.

Stone, E. J., & Lunt, D. J. (2013). The role of vegetation feedbacks on greenland glaciation. *Climate dynamics*, *40*(11), 2671–2686.

Sueyoshi, T., Ohgaito, R., Yamamoto, A., Chikamoto, M., Hajima, T., Okajima, H., ... others (2013). Set-up of the pmip3 paleoclimate experiments conducted using an earth system model, miroc-esm. *Geoscientific Model Development*, *6*(3), 819–836.

Tarasov, L., Dyke, A. S., Neal, R. M., & Peltier, W. (2012b, jan). A data-calibrated distribution of deglacial chronologies for the North American ice complex from glaciological modeling. *Earth and Planetary Science Letters*, *315-316*, 30–40. Retrieved from https://www.sciencedirect.com/science/article/pii/S0012821X11005243 doi: 10.1016/J.EPSL.2011.09.010

Tarasov, L., Dyke, A. S., Neal, R. M., & Peltier, W. R. (2012a). A data-calibrated distribution of deglacial chronologies for the north american ice complex from glaciological modeling. *Earth and Planetary Science Letters*, *315*, 30–40.

Tierney, J. E., Zhu, J., King, J., Malevich, S. B., Hakim, G. J., & Poulsen, C. J. (2020). Glacial cooling and climate sensitivity revisited. *Nature*, *584*(7822), 569–573.

Tulenko, J. P., Lofverstrom, M., & Briner, J. P. (2020). Ice sheet influence on atmospheric circulation explains the patterns of pleistocene alpine glacier records in north america. *Earth and Planetary Science Letters*, *534*, 116115.

Ullman, D., LeGrande, A., Carlson, A. E., Anslow, F., & Licciardi, J. (2014). Assessing the impact of laurentide ice sheet topography on glacial climate. *Climate of the Past*, *10*(2), 487–507.

Vernon, C. L., Bamber, J., Box, J., Van den Broeke, M., Fettweis, X., Hanna, E., & Huybrechts, P. (2013). Surface mass balance model intercomparison for the greenland ice sheet. *The Cryosphere*, *7*(2), 599–614.

Vizcaíno, M., Lipscomb, W. H., Sacks, W. J., van Angelen, J. H., Wouters, B., & van den Broeke, M. R. (2013). Greenland surface mass balance as simulated by the community earth system model. part i: Model evaluation and 1850–2005 results. *Journal of climate*, *26*(20), 7793–7812.

Voldoire, A., Sanchez-Gomez, E., Salas y Mélia, D., Decharme, B., Cassou, C., Sénési, S., ... others (2013). The cnrm-cm5. 1 global climate model: description and basic evaluation. *Climate dynamics*, *40*(9), 2091–2121.

Williamson, D. (2015). Exploratory ensemble designs for environmental models using k-extended latin hypercubes. *Environmetrics*, *26*(4), 268–283.

Ziemen, F. A., Rodehacke, C. B., & Mikolajewicz, U. (2014, oct). Coupled ice sheet–climate modeling under glacial and pre-industrial boundary conditions. *Climate of the Past*, *10*(5), 1817–1836. Retrieved from https://www.clim-past.net/10/1817/2014/ doi: 10.5194/cp-10-1817-2014